SIMULATIONS FOR STEAM METHANE REFORMING OVER Ni/Al_2O_3 CATALYST IN A FIXED BED REACTOR AND A MEMBRANE REACTOR

CHAN KIT YEN

UNIVERSITI SAINS MALAYSIA

2021

SIMULATIONS FOR STEAM METHANE REFORMING OVER Ni/Al_2O_3 CATALYST IN A FIXED BED REACTOR AND A MEMBRANE REACTOR

by

CHAN KIT YEN

Thesis submitted in partial fulfilment of the requirement

for the degree of Bachelor of Chemical Engineering

July 2021

ACKNOWLEDGEMENT

First of all, I would like to express my utmost gratitude to my respectful supervisor, Associate Professor Dr. Tye Ching Thian, who guided me through this final year project. She is willing to supervise the project's progress and share with me her knowledge in spite of her hectic schedule. I sincerely appreciate her support, guidance, motivation and knowledge throughout the whole process to project completion.

Apart from that, I would like to thank my beloved family and friends for their unceasing support and encouragement throughout the whole project completion. Once again, I would like to thank to those whom I might have missed out who have helped me directly and indirectly. Their contributions are very much appreciated.

CHAN KIT YEN

July 2021

TABLE OF CONTENTS

LIST OF TABLES

LIST OF FIGURES

LIST OF SYMBOLS

Symbol	Description	Unit
X_{CH_4}	Conversion of CH_4	
X_{CO_2}	Conversion of CO_2	
Y_{H_2}	Yield of H_2	mol H_2/mol CH_4
S_{CO_2}	Selectivity of CO_2	
S_{CO}	Selectivity of CO	
δ	Membrane thickness	μm
L	Length of catalyst bed	m
A_C	Cross-sectional area of reaction zone of reactor	
$F^0_{CH_4}$	Methane inlet molar flow rate	kmol/h
r_1	Rate of formation of CH_4 in steam methane reforming reaction	kmol/h
r_2	Rate of formation of CO in water-gas shift reaction	kmol/h
r_3	Rate of formation of CH_4 in reverse methanation reaction	kmol/h
P_{perm}	Permeate zone pressure	bar

LIST OF ABBREVIATIONS

SMR	Steam methane reforming
S/C	Steam/methane feed ratio
Ni	Nickel catalyst
FBR	Fixed Bed Reactor
MR	Membrane Reactor
Pd/SS membrane	Palladium/porous stainless steel composite membrane
WGS	Water gas-shift

SIMULATIONS FOR STEAM METHANE REFORMING OVER Ni/Al_2O_3 CATALYST IN A FIXED BED REACTOR AND A MEMBRANE REACTOR

ABSTRACT

The limitations of steam methane reforming (SMR) process in fixed bed reactor (FBR) is thermodynamic equilibrium constraint and the requirement of high operating temperature. Membrane reactor (MR) have huge application potential for the equilibrium limited, endothermic SMR process due to the simultaneous withdrawal of reaction product, H_2. The steady-state behavior of SMR process in FBR and MR are examined by developing a 1-D, pseudo-homogeneous mathematical modelling framework that operates at isothermal and isobaric mode. The calculation procedures was performed using MATLAB and both of the reactor models were validated against experimental data. Comparative SMR performance assessment in terms of methane conversion (X_{CH_4}), H_2 yield and selectivity of CO (S_{CO}) and CO_2 (S_{CO_2}) between FBR and MR were accordingly conducted. The increasing temperature has positive impact on X_{CH_4} and H_2 yield, but at temperature above 650 ℃, the positive impact of H_2 removal in MR becomes less significant compared to FBR. Besides, S_{CO_2} and S_{CO} are only affected by temperature in which increasing temperature promotes the reverse water gas shift reaction, resulting in the increase of S_{CO}. For FBR, S_{CO} exceeds S_{CO_2} at around 590 ℃ while for MR, S_{CO} exceeds S_{CO_2} at around 610 ℃. Next, the effect of increasing reaction pressure show an opposite trend for MR and FBR, in MR, higher X_{CH_4} is obtained when pressure increases due to the increase of H_2 partial pressure driving force but in FBR, higher pressure is not favoured. In addition, methane inlet flow rate higher than 0.03 kmol/h suppressed the positive impact of H_2 removal in MR while lower permeation zone pressure (P_{perm}) and higher sweep gas flow rate improve the reaction performance in MR.

SIMULASI TERHADAP STIM METANA PEMBENTUKAN SEMULA DENGAN MANGKIN Ni/Al_2O_3 DALAM REAKTOR LAPISAN-TETAP DAN REAKTOR MEMBRAN

ABSTRAK

Batasan proses pembaharuan metana wap (SMR) dalam reaktor lapisan-tetap (FBR) adalah kekangan keseimbangan termodinamik dan keperluan suhu operasi yang tinggi. Reaktor membran (MR) mempunyai potensi besar untuk proses SMR yang bersifat endotermik dan keseimbangan terhad dengan pemisahan produk tindak balas, H_2. Perilaku keadaan mantap proses SMR dalam FBR dan MR diperiksa dengan mengembangkan kerangka pemodelan matematik 1-D, pseudo-homogen yang beroperasi pada mod isoterma dan isobarik. Prosedur pengiraan dilakukan menggunakan MATLAB dan kedua-dua model reaktor itu disahkan berdasarkan data eksperimen. Penilaian prestasi SMR perbandingan dari segi penukaran metana (X_{CH_4}), hasil H_2 dan selektivitas CO (S_{CO}) dan CO_2 (S_{CO_2}) antara FBR dan MR telah dilakukan. Kesan peningkatan suhu memberi kesan positif pada SMR tetapi pada suhu lebih 650 ℃, kesan positif pemisahan H_2 di MR menjadi kurang ketara berbanding FBR. Selain itu, S_{CO_2} dan S_{CO} hanya dipengaruhi oleh suhu di mana suhu yang lebih tinggi mendorong reaksi pergeseran stim gas terbalik, yang mengakibatkan peningkatan S_{CO}. Untuk MR, S_{CO} melebihi S_{CO_2} sekitar 590 ℃ sementara untuk FBR, S_{CO} melebihi S_{CO_2} sekitar 610 ℃. Seterusnya, kesan peningkatan tekanan reaksi menunjukkan tren yang berlawanan untuk MR dan FBR, di MR, X_{CH_4} yang lebih tinggi diperoleh apabila tekanan meningkat disebabkan oleh peningkatan daya penggerak tekanan separa H_2 tetapi di FBR, tekanan yang lebih tinggi tidak disukai. Di samping itu, kadar aliran masuk metana lebih tinggi daripada 0.03 kmol/j menekan kesan positif penyingkiran H_2 di MR sementara P_{perm} yang lebih rendah dan kadar aliran gas sapuan yang lebih tinggi meningkatkan prestasi tindak balas di MR.

CHAPTER 1
INTRODUCTION

1.1 Research background

Synthesis gas (syngas) is a gas mixture that consists of H_2, CO and CO_2 as main component, it is a key intermediate for the syntheses of various chemicals and fuels, as well as the source of pure H_2 and CO. Basically, syngas production serves two markets, firstly, the supply of H_2 to fertiliser industry for ammonia synthesis, next, H_2 is also an essential feedstock for oil refining and the production of various petrochemicals. In addition, H_2 has been widely acknowledged as a clean energy carrier and considerable research attention has drawn on the development of fuel cell using hydrogen as green energy carrier. Secondly, CO gas mixture is the supply for the production of methanol, Fischer-Tropsch liquids and other chemicals.

The standard process to produce syngas on an industrial scale is steam methane reforming (SMR), in which the feedstock is natural gas with methane as primary component (the higher hydrocarbons in natural gas will be converted to methane in SMR). This tendency will still remain in the future because of the wide availability of natural gas. Industrial SMR is carried out in multiple high-alloy reforming tubes packing with catalyst pellets and placed within a furnace with operating temperatures ranging from 700 °C to 1000 °C and pressure above 30 bar (Gil, 2015). Usually after SMR, CO in the product stream will be further reduced in the high and low temperature water-gas shift (WGS) adiabatic reactors to enrich the gas mixture in H_2. After that, H_2 is separated from the gas mixture in pressure swing adsorption units (Pantoleontos et al., 2012).

Since methane molecule is very stable and resistant to many reactants, catalysts are essential to accomplish SMR at the practical range of temperatures. Supported nickel (Ni) catalysts are the most abundantly used catalysts in SMR. Although other transition metals such as platinum, palladium and ruthenium are more active per unit weight, yet Ni is significantly

cheaper with its catalytic activity not significantly affected (Norris, 2013). The most common supports used in the open literature for SMR are α-Al_2O_3 , γ- Al_2O_3 , SiO_2, MgO, $MgAl_2O_4$, CeO_2, TiO_2 and ZrO_2. α-Al_2O_3 and γ- Al_2O_3 are the most common support for SMR as it is inexpensive and easy to prepare (Nieva et al., 2014). The difference between Ni-α-Al_2O_3 and Ni-γ- Al_2O_3 is that Ni-γ- Al_2O_3 will becomes unstable at temperature above 700 °C and undergo phase transform into α-Al_2O_3 due to thermal deterioration of γ- Al_2O_3 that results in pore blockage and sintering, thereby reduce the surface area of catalytic activity.

Due to the highly endothermic nature of SMR, the overall performance relies on an efficient heat management of the process. Due to the lower energy consumption, easier design and lower operating costs, membrane reactors (MR) that combine chemical reaction and membrane separation in a single unit have emerged as a viable option to reduce the drastic operating temperature of conventional industrial SMR. The development of inorganic membranes such as palladium (Pd) membrane with good thermal stability and 100 % selectivity towards H_2 has gained attention to the application to high temperature chemical reactions such as SMR. Besides achieving high methane conversion, pure H_2 can also be obtained by H_2 permeation through the membrane. Although H_2 is reported to have higher solubility in other metal membranes such as Niobium, Tantalum and Vanadium, the formation of an oxide layer will lead to malfunction of these membranes, limiting their practical use. Porous stainless steel (SS) supported Pd membrane are mechanically and chemically stable, most importantly, the membrane thickness can be significantly reduced, resulting in higher H_2 permeation and lower material cost (Gil, 2015).

1.2 Problem Statement

The main restriction for SMR process is thermodynamic equilibrium constraint in which the conversion approaches its maximum at a specific reaction temperature and pressure. (A.M. Adris, 1996). The equilibrium-limited reactions are thermodynamically governed by the Le Chatelier's principle, which states that when a reaction system is subjected to a change in either concentration, temperature or pressure, the system readjusts itself to counteract the effect of the applied change to establish a new equilibrium (Gil, 2015). Since the overall SMR reactions is endothermic and generate more molar of product molecules than reactants, it is thermodynamically favoured at high temperature and low pressure. Conventional industrial SMR is usually carried out in FBR at high temperature between 700 to 1000 °C. Although low pressure favours the reactant conversion, pressure higher than 20 bar is always chosen because it is desirable by H_2 end users such ammonia synthesis and it also allows more compact reactor design (Khzouz, 2014). The thermodynamic limitations makes the whole SMR process very energy intensive.

MR have huge application potential for the equilibrium limited, endothermic SMR process because the in situ withdrawal of reaction product, H_2 can avoid the achievement of equilibrium conversion by shifting the reaction equilibrium to the product side thereby increase of methane conversion. Moreover, by using MR, the drastic operating temperature that usually used by conventional fixed bed reactor (FBR) can be lowered but high methane conversion still can be achieved. This can lower the heat duty requirement and thus the fuel consumption that used to generate high reaction temperature. In addition, ultrapure H_2 can be obtained by membrane separation from the reaction gas. Usually, the reaction zone is configured as shell side while permeation zone is in the inner membrane tube (De Falco et al., 2014). This is for the reason that the SMR is endothermic which requires heat supply from the furnace to the outer reactor wall and then to the reaction zone at shell side.

In this study, simulation of fixed bed and membrane reactor are conducted by using MATLAB. Chemical processes simulators is an important tools for modelling chemical processes and providing opportunities for optimization and debottlenecking of the existing process. Sophisticated simulators with high accuracy have been developed but many of these take a long time to converge, making it impractical for continuous prediction of process parameters especially for industrial use (Zečević and Bolf, 2020). When dealing with the simulation of steady-state reactors, pseudo-homogeneous plug-flow model is generally considered adequate due to their convenient mathematical formulation (Costamagna et al., 2020). Hence, a 1-D, pseudo-homogeneous, isothermal and isobaric reactor models for MR and FBR respectively are going to be simulated in this work. The effect of operating parameters which are reaction temperature, pressure, steam/methane feed ratio, reactants residence time, sweep gas/methane ratio as well as permeate zone pressure are studied using the model developed and validated with experimental results. The SMR reaction performance based on methane conversion, H_2 yield as well as the selectivity of product, CO and CO_2 respectively are compared between MR and FBR.

1.3 Objectives

The objectives of this study are:

i. To simulate an isothermal one-dimensional model for fixed bed reactor and membrane reactor.

ii. To study and compare the effect of temperature, pressure, steam/methane feed molar ratio, methane feed molar flow rate, sweep gas ratio and permeation zone pressure on SMR reaction.

iii. To compare the SMR reaction performance in a MR and a FBR.

CHAPTER 2

LITERATURE REVIEW

This chapter surveyed the recent research carried out for SMR simulation in MR and FBR as well as the development of catalyst to enhance SMR performance.

2.1 Simulation of SMR in Fixed Bed Reactor

Latham (2008) had developed an industrial SMR mathematical model for process simulations use and on-line monitoring of reformer tube-wall temperature profiles and reaction gas composition profile. Since industrial reformer consists of furnace to supplies heat energy to reformer tube where SMR reactions occur, Latham had simulated both furnace and reactor side by divided them into 20 discrete zones of uniform temperature and composition. The goal was to generate the outer-reformer-tube-wall temperature using minimal computation time to mitigate the risk of tube failure. It is for the reason that an increase of 20 ℃ than the tube design temperature can reduce the tube life expectancy by half for a given alloy, thus, over time creep can cause reformer tube failure thereby requires costly tube replacements, plant shut downs and production losses. Non-linear algebraic mass and energy conservation laws equations were performed on each zone and solved iteratively with Newton-Raphson method. Radiative heat transfer in furnace was model by using Hottel Zone method. The total exchange area was calculated by using RADEX program. The inputs of the simulation include furnace geometry and material properties, catalyst properties as well as SMR feed properties. Starting from a reasonable initial guess that can be obtained from plant data, the model has a solution time less than 4 minutes.

Pantoleontos et al. (2012) used an equation-based software platform gPROMS 3.4 to examine the dynamic behaviour of a heterogeneous SMR process in FBR, accounting for the diffusional limitations within catalyst pellets. Non-constant effectiveness factors (η) which

vary with time and along the axial direction were calculated by the transport equations in the catalyst particles, proving that the process is diffusion-limited which cannot be treated as homogeneous. Second-order spatial derivatives and accumulation terms were included in the model. The heat provided to the reactor was optimised in term of optimal H_2 yield by using a quadratic temperature profile. The optimisation parameters were solved under steady-state conditions and then applied to the dynamic model. Concentration and temperature profiles along the axial direction and time were generated using the dynamic model.

2.2 Simulation of SMR in Membrane Reactor

De Falco et al. (2014) had performed heat duty assessment of SMR process in MR with Pd-Ag/SS membrane by simulation to determine how the main operating parameters such as temperature, pressure, steam/methane feed ratio (S/C) and reactant space velocity influence the total heat power requirement. The simulation results showed that the thermal energy required for the production and separation of 1 kmol of pure H_2 decreases as temperature increases, which is from 222.7 kWh/kmol (400 ℃) to 176.6 kWh/kmol (600 ℃). Besides, although higher S/C has a slight positive effect on methane conversion (X_{CH_4}), yet it imposed a stronger negative impact on the reactant steam generation heat duty. Next, as the reactants space velocity increases from 2 kmol/h to 7 kmol/h, the total heat power required increases from 683 kW to 1056 kWh due to the higher steam generation, yet, the reaction performance is poorer due to the reduction of reactants residence time. A pie chart reported the heat duty sharing at the optimal MR operating condition (600 ℃, 25 bar, methane inlet flow rate = 2 kmol/h, S/C = 2.5 and sweep gas/methane ratio = 1) are shown in Figure 2.1. The pie chart shows that 80 % of the heat duty is consumed by the endothermic SMR reaction while 10 % is consumed by reactant steam generation. An almost complete methane conversion is also achieved at 600 ℃,

a much lower temperature than conventional SMR reformer temperature, showing the huge potential of MR.

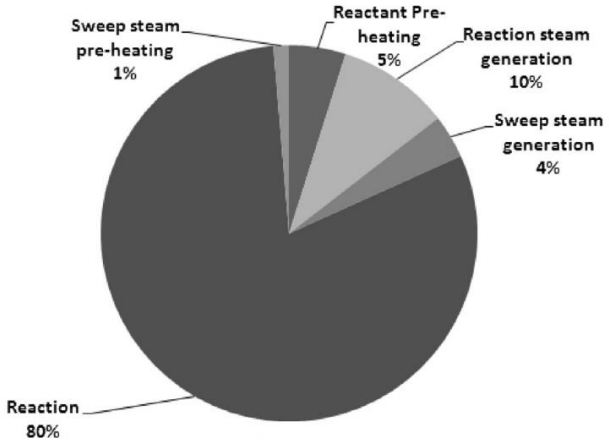

Figure 2.1: Heat duty sharing of a membrane reactor simulated by De Falco et al. (2014).

Gallucci et al. (2006) had investigated the influence of different retentate and permeate flux configurations which are co-current and counter-current mode on X_{CH_4} and H_2 recovery using a Pd-Ag membrane. The simulation results showed that counter-current mode gave higher X_{CH_4} and H_2 recovery than co-current mode. With the shell side as permeation zone and tube side as reaction zone, Figure 2.2 and 2.3 below showed the H_2 partial pressure profile along the reactor length. For co-current mode (Figure 2.2), the H_2 partial pressure difference between reaction and permeation zone becomes smaller as reactor distance increases, consequently, H_2 permeation would stop when the H_2 partial pressure difference is zero and thus it is impossible to recover all H_2 from the reaction gas. For counter-current mode (Figure 2.3), there is a constant H_2 partial pressure difference between reaction and permeation zones, which means driving force for H_2 permeation will always present. Therefore, with sufficient long reactor length, total H_2 recovery is possible, equilibrium limitations can be completely overcome and complete methane conversion can be achieved.

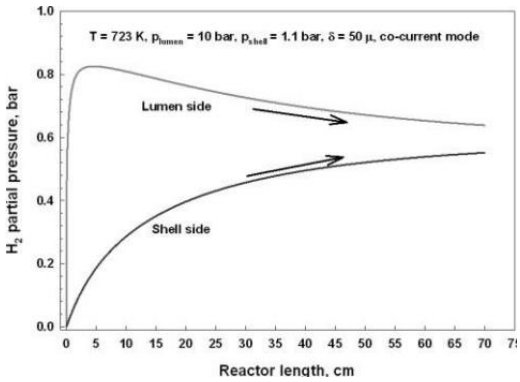

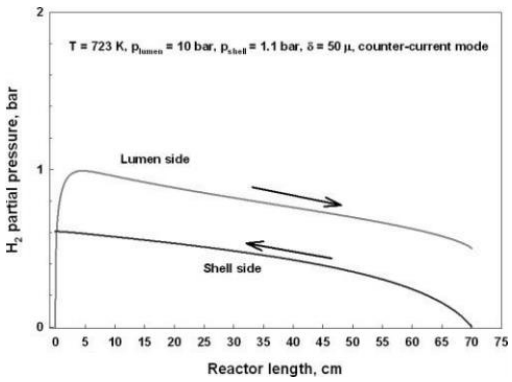

Figure 2.2: Co-current mode membrane reactor. Figure 2.3: Counter-current mode membrane reactor.

2.3 Development of Different Catalyst to Improve SMR Performance

Khzouz (2014) had done modification on Ni/Al_2O_3 catalyst using copper (Cu) as promoter metal to enhance stability of catalyst as well as decomposition of methane. The theory behind this is that Cu promoter dilute the Ni surface atoms thus decrease the amount of adsorbed carbon thereby minimize the carbon formation rate. SMR experiments are conducted using various loading of Ni/Cu (7%Ni-3%Cu, 5%Ni-5%Cu and 3%Ni-7%Cu), 10%Ni (without Cu) and 10%Cu (without Ni) are served as control sets for comparison, the experiments are conducted at S/C of 3 from 500 to 700 ℃. The results shows that only 7%Ni-3%Cu displayed higher X_{CH_4} and H_2 yield than 10%Ni and other Ni/Cu loadings starting from 600 ℃. Below 600 ℃ 10%Ni gave the highest X_{CH_4} compared to other catalyst loadings. The main reactions of SMR scheme are shown below, reaction (2.1) and (2.3) are endothermic while reaction (2.2) is exothermic, comprising an overall endothermic set:

$CH_4 + H_2O \leftrightarrow CO + 3H_2$ (2.1) Steam methane reforming reaction

$CO + H_2O \leftrightarrow CO_2 + H_2$ (2.2) Water-gas shift reaction

$CH_4 + 2H_2O \leftrightarrow CO_2 + 4H_2$ (2.3) Reverse methanation

The result showed that there was no methane conversion detected over the 10% Cu catalyst, thereby it is postulated that Cu is responsible in enhancing water gas-shift (WGS) reaction only. At the loading of 7%Ni-3%Cu, Ni surface area is larger, leading to higher X_{CH_4} resulted from reaction (2.1) and (2.3) meanwhile, CO produced by reaction (2.1) is consumed and enhanced by Cu in reaction (2.2), further increasing X_{CH_4} as SMR reaction equilibrium is shifted to the right when more CO is consumed. At temperature above 600 ℃, 7%Ni-3%Cu catalyst only displayed a slightly higher X_{CH_4} and H_2 yield than 10%Ni, due to the exothermic nature of WGS reaction. This means that Cu catalyst at high temperature favours reverse water gas-shift reaction, producing more CO and less H_2.

Xu et al. (2008) had investigated the effect ceria (CeO_2) deposition to commercial $Ni/SiO_2/Al_2O_3$ catalyst on the reduction of carbon deposition under low S/C of 1.3 and 0.25 using different deposition methods which are deposition precipitation and sol-gel method. S/C higher than 3 is usually used in industrial SMR to achieve higher X_{CH_4}, another reason is that low S/C lower will cause Ni catalyst to suffer from severe carbon deposition. By using S/C higher than 1, the deposited carbon can be removed through gasification with steam or CO_2. However, the usage of high S/C not only requires more energy input but will also dilute the H_2 content at product gas. Thus, economic implications tend to favour the use of lower S/C by developing new catalysts which resist carbon formation. The results of Xu et al. (2008) showed that sol-gel method using cerium alkoxide appeared to be the most effective method in which under a highly reducing condition of 800 ℃ and S/C = 0.25, a constant 25 % X_{CH_4}, indicating total consumption of steam was observed for more than 5 days (112 hours) of operation. Under the same experimental condition, commercial $Ni/SiO_2/Al_2O_3$ catalyst (without CeO_2 deposition) lost all its activity for H_2 production within 5 hours with the reactor entirely blocked up by carbon depositions. CeO_2 is known for its carbon deposition resistance due to its redox activity.

It is postulated that CeO_x prevent carbon accumulation by accelerating the reaction of steam with adsorbed carbon at the metal-oxide interface so that methane can be converted into products quickly.

CHAPTER 3

METHODOLOGY

This chapter discussed the methods applied in this final year project, including the general research flow diagram, formulation of mathematical equations for the simulation of fixed bed reactor (FBR) and membrane reactor (MR), kinetic model adopted from literature and the use of MATLAB.

3.1 Overview of Research Methodology

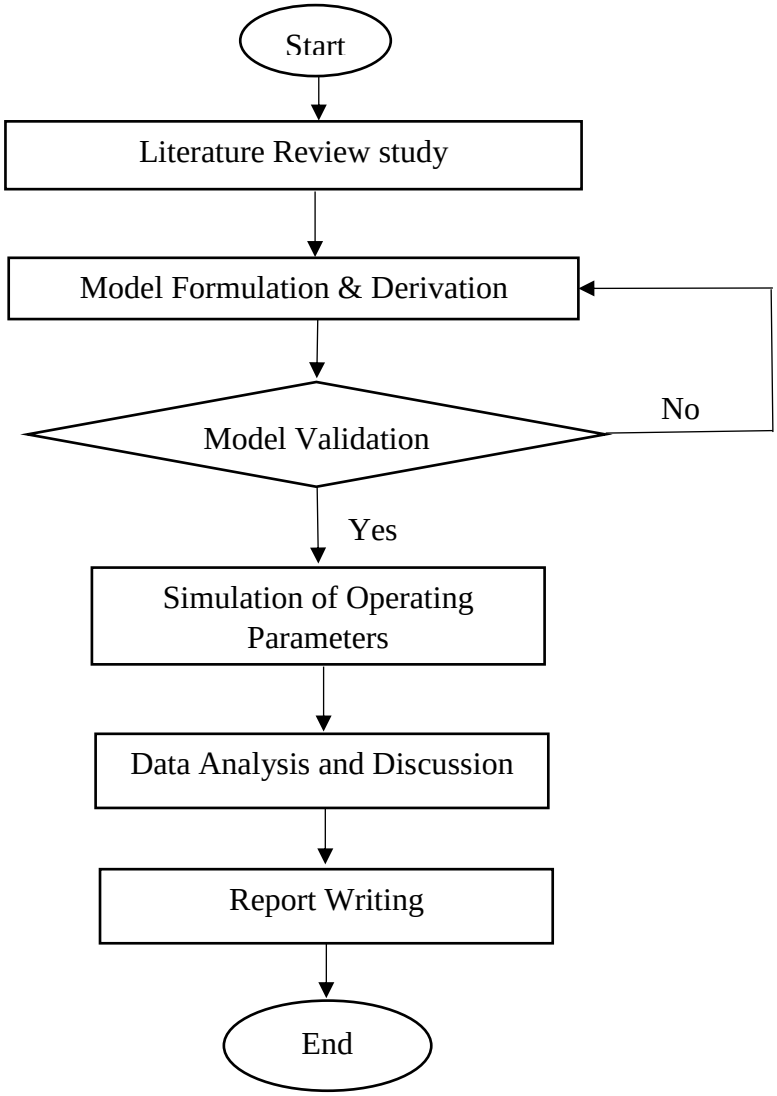

Figure 3.1 Flow chart of simulation research activities.

3.2 Reactor Model Development

SMR in a fixed bed reactor (FBR) and a membrane reactor (MR) are simulated. The models are validated based on the experimental data reported by Shu et al. (1994). The reactor is fixed in the middle of the furnace to maintain a uniform temperature distribution. The simulations of both MR and FBR includes the formulation of general equations based on law of conservation of mass. The model is one-dimensional, isothermal, isobaric and steady state due to the small dimension of reactors. Although these simplifications may be far from the industrial case, the model helps to get a range of experimental result where we can increase or decrease the range when suppressing the simplifications made.

According to Xu and Froment (1989) and other literature data (Zečević and Bolf, 2020), only 3 reactions are critical for thermodynamic and kinetic consideration for SMR process, which are:

$CH_4 + H_2O \leftrightarrow CO + 3H_2$ (2.1) Steam methane reforming reaction

$CO + H_2O \leftrightarrow CO_2 + H_2$ (2.2) Water-gas shift reaction

$CH_4 + 2H_2O \leftrightarrow CO_2 + 4H_2$ (2.3) Reverse methanation

Reactions (2.1) and (2.3) are highly endothermic while reaction (2.2) is mildly exothermic, overall, SMR reactions is highly endothermic. In general condition, the presence of 3 reactions requires 3 sets of differential equations.

3.2.1 Model Assumptions

In the model derived, the following assumptions are made:

i. Pseudo-homogeneous model

ii. Negligible radial variation in temperature and concentration

iii. Isothermal condition

iv. Negligible pressure drop

v. The reaction gas mixture follows ideal gas law

vi. Steady state operation

vii. No carbon formation from side reaction

3.2.2 Fixed Bed Reactor

The fixed bed reactor (FBR) consists of an outer stainless steel (SS) tube and an inner SS tube. Figure below is the schematic drawing of the FBR, it can be configured to membrane reactor (MR) by replacing the SS inner tube with Palladium/porous stainless steel composite (Pd/SS) membrane.

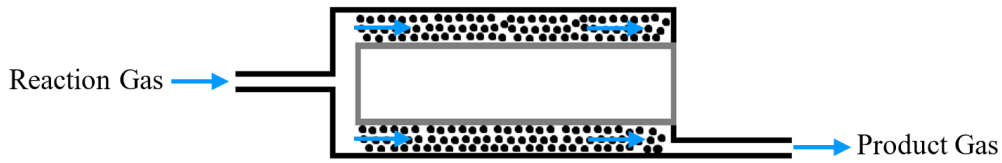

Figure 3.2 Schematic diagram of SMR in fixed bed reactor.

The dimensions of FBR as well as other related parameters used in this simulation followed the experiment conducted by Shu et al. (1994), which is tabulated in Table 3.1 below.

Table 3.1: Reactor parameters and constants of FBR.

Properties	Dimension (unit)
Inner radius of outer reactor tube, R	0.85 cm
Length of catalyst bed, L	3.6 cm
Outer radius of SS inner tube, $r_{m,in}$	0.475 cm
Thickness of SS inner tube, δ	19.8 μm
Density of catalyst, ρ_{cat}	1870 kg/m^3
Weight of catalyst, W	0.011 kg
Methane inlet molar flow, $F_{CH_4}^0$	0.00034 kmol/h

Hence, the cross-sectional of the reaction zone, A_C is defined by:

$$A_C = \pi\left[R^2 - {r_{m,in}}^2\right]$$

The first step towards reactor modelling is by applying law of conservation of mass over a catalyst weight ΔW, Figure 3.2 shows an illustration of the flow of reactant (F_A) over ΔW in a FBR.

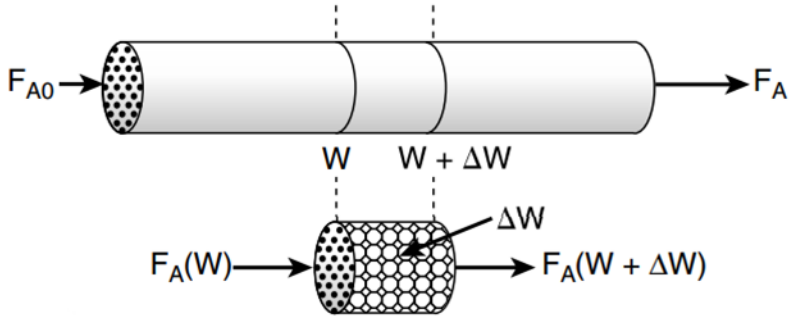

Figure 3.3: Illustration of reactant flow over a weight of catalyst in a FBR.

The mass balance at the reaction zone is started from the generalized mole balance equation:

$$\left[\begin{matrix}Rate\ of\ flow\\ of\ A\ into\ the\\ system\\ (moles/time)\end{matrix}\right] - \left[\begin{matrix}Rate\ of\ flow\\ of\ A\ out\ of\\ the\ system\\ (moles/time)\end{matrix}\right] + \left[\begin{matrix}Rate\ of\ generation\\ of\ A\ by\ chemical\\ reaction\ within\ the\\ system\\ (moles/time)\end{matrix}\right] = \left[\begin{matrix}Rate\ of\\ accumulation\\ of A\ within\ the\\ system\\ (moles/time)\end{matrix}\right]$$

In $-$ Out $+$ Generation $=$ Accumulation

$$F_{A0} - F_A + G_A = \frac{dN_A}{dt} \qquad (3.1)$$

At steady-state, $\frac{dN_A}{dt} = 0$

$$F_{A|W} - F_{A|(W+\Delta W)} + r_A \Delta W = 0 \qquad (3.2)$$

Where ΔW = catalyst weight (kg_{cat})

r_A = rate of formation of species A (kmol/ kg_{cat} s)

Divide by ΔW and rearranging, equation (3.2) becomes:

$$\left[\frac{F_{A|(W+\Delta W)} - F_{A|W}}{\Delta W}\right] = r_A \qquad (3.3)$$

Take the limit as ΔW approaches zero, $\lim_{\Delta W \to 0} \left[\frac{F_{A|(W+\Delta W)} - F_{A|W}}{\Delta W}\right] = \frac{dr_A}{dW}$, equation (3.3) becomes:

$$\frac{dF_A}{dW} = r_A \tag{3.4}$$

The weight of catalyst term (W) is replaced with bulk catalyst density (ρ_b), cross-sectional area of catalyst bed (A_C) and length of catalyst bed (L), yielding equation (3.5):

$$\rho_b \left(\frac{kg_{cat}}{m^3}\right) = \frac{W\ (kg_{cat})}{A_C\ (\mathrm{m}^2) \cdot L(m)}$$

$$dW = \rho_b A_C dL$$

$$\frac{dF_A}{dL} = r_A\ \rho_b\ A_C \tag{3.5}$$

Replace dL with dimensionless reactor length (dL^*) where $dL^* = dL/L$,

$$\frac{dF_A}{dL^*} = r_A\ \rho_b L A_C \tag{3.6}$$

There are 5 species in this SMR process, which are CH_4, H_2O, H_2, CO and CO_2. CH_4 and H_2O are consumed by the reactions while H_2, CO and CO_2 are generated from the reactions aforesaid in section 3.2. The molar flow rate of each species is derived as:

$$\frac{dF_{\mathrm{CH_4}}}{dL^*} = -r_{\mathrm{CH_4}}\ \rho_b L A_C = (-r_1 - r_3)\ \rho_b L A_C \tag{3.7}$$

$$\frac{dF_{\mathrm{H_2O}}}{dL^*} = -r_{\mathrm{H_2O}}\ \rho_b L A_C = (-r_1 - r_2 - 2r_3)\ \rho_b L A_C \tag{3.8}$$

$$\frac{dF_{\mathrm{H_2}}}{dL^*} = r_{\mathrm{H_2}}\ \rho_b L A_C = (3r_1 + r_2 + 4r_3)\ \rho_b L A_C \tag{3.9}$$

$$\frac{dF_{\mathrm{CO}}}{dL^*} = r_{\mathrm{CO}}\ \rho_b L A_C = (r_1 - r_2)\ \rho_b L A_C \tag{3.10}$$

$$\frac{dF_{\mathrm{CO_2}}}{dL^*} = r_{\mathrm{CO_2}}\ \rho_b L A_C = (r_2 + r_3)\ \rho_b L A_C \tag{3.11}$$

Methane conversion, X_{CH_4} is defined as:

$$X_{CH_4} = \frac{F^0_{CH_4} - F_{CH_4}}{F^0_{CH_4}} \tag{3.12}$$

Rearrange eq. (3.12),

$$F_{CH_4} = F^0_{CH_4}(1 - X_{CH_4}) \tag{3.13}$$

Substitute eq. (3.13) to (3.7)

$$\frac{dF^0_{CH_4}(1 - X_{CH_4})}{dL^*} = (-r_1 - r_3)\,\rho_b L A_C$$

$$\frac{d(1-X_{CH_4})}{dL^*} = \frac{\rho_b L A_C}{F^0_{CH_4}}(-r_1 - r_3)$$

$$\frac{dX_{CH_4}}{dL^*} = -\frac{\rho_b L A_C}{F^0_{CH_4}}(-r_1 - r_3) = \frac{\rho_b L A_C}{F^0_{CH_4}}(r_1 + r_3) \tag{3.14}$$

Conversion of CO_2 (X_{CO_2}) is defined as:

$$X_{CO_2} = \frac{F_{CO_2}}{F^0_{CH_4}} \tag{3.15}$$

Rearrange eq. (3.15),

$$F_{CO_2} = X_{CO_2} F^0_{CH_4} \tag{3.16}$$

Substitute eq. (3.16) to (3.11),

$$\frac{dX_{CO_2}}{dL^*} = \frac{\rho_b L A_C}{F^0_{CH_4}}(r_2 + r_3) \tag{3.17}$$

The performance of FBR is evaluated by the conversion of CH_4 (X_{CH_4}), yield of H_2 (Y_{H_2}), Selectivity of CO (S_{CO}) and selectivity of CO_2 (S_{CO_2}), which are defined by:

$$X_{CH_4} = \frac{F^0_{CH_4} - F_{CH_4}}{F^0_{CH_4}} \times 100\% = \frac{\rho_b L A_C}{F^0_{CH_4}}(r_1 + r_3) \times 100\% \tag{3.20}$$

$$Y_{H_2} = \frac{F_{H_2}}{F^0_{CH_4}} \quad (3.21)$$

$$= \frac{\rho_b L A_C}{F^0_{CH_4}} (3r_1 + r_2 + 4r_3) \quad (3.22)$$

$$S_{CO_2} = \frac{F_{CO_2}}{F_{CO_2}+F_{CO}} \times 100\% \quad (3.23)$$

$$S_{CO} = \frac{F_{CO}}{F_{CO_2}+F_{CO}} \times 100\% \quad (3.24)$$

3.2.3 Membrane Reactor

Figure below shows the schematic drawing of the membrane reactor (MR), the shell side is the reaction zone packed with Ni/Al_2O_3 catalyst while tube side is the permeate zone.

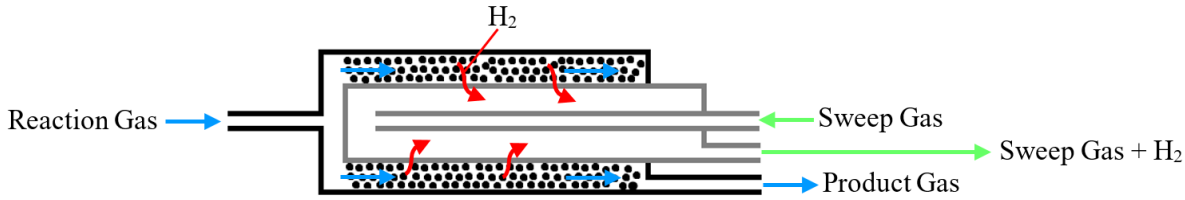

Figure 3.4: Schematic drawing of SMR in membrane reactor.

The dimensions of reactors, permeate zone pressure and sweep gas ratio are tabulated in Table 3.2 below.

Table 3.2: Reactor parameters and constants of MR.

Properties	Dimension (unit)
Inner radius of fixed bed reactor tube, R	0.85 cm
Length of catalyst bed, L	3.6 cm
Outer radius of Pd/SS membrane, $r_{m,in}$	0.475 cm
Thickness of Pd/SS membrane, δ	19.8 μm
Density of catalyst, ρ_{cat}	1870 kg/m^3
Weight of catalyst, W	0.011 kg

Methane inlet molar flow, $F_{CH_4}^0$	0.00034 kmol/h
Sweep gas flow rate, F_{Sweep}	0.00034 kmol/h
Permeate zone pressure, P_{Perm}	1 bar

Hence, the cross-sectional of the reaction zone, A_C is defined by:

$$A_C = \pi\left[R^2 - {r_{m,in}}^2\right]$$

Reaction Zone

The mass balance derivation across MR is the same as those in FBR derived in the previous section, refer equation (3.1) to (3.17).

Permeate Zone

Pd/SS membrane is only permeable to H_2, Fick's first law of diffusion is used to describe the mass transfer of H_2 permeating through the Pd/SS membrane:

$$J_{H_2} = -D\frac{dC_{H_2}}{\mathrm{dx}} \tag{3.25}$$

Where J_{H_2} = molar flux of H_2 through the membrane ($mol/m^2 \cdot s$);

D = diffusion coefficient (m^2/s);

$\frac{dC_{H_2}}{\mathrm{dx}}$ = concentration gradient across the membrane thickness.

δ = membrane thickness, assuming a constant D,

Equation (3.25) is integrated into:

$$J_{H_2} = D\frac{(C_{H_2}^{ret} - C_{H_2}^{perm})}{\delta} = D\frac{\Delta C}{\delta} \tag{3.26}$$

Where $C_{H_2}^{ret}$ = concentration of H_2 at the retentate side (reaction zone)

$C_{H_2}^{perm}$ = concentration of H_2 at the permeate side

The sorption isotherm of Pd and Pd-alloy membrane, which is in the category of metal membrane, is usually described by Sievert's Law (Campo et al., 2011):

$$C_{H_2} = k_{H_2}\left(P_{H_2}\right)^{0.5} \tag{3.27}$$

Where k_{H_2} = Sievert's constant; P_{H_2} = partial pressure of H_2

Thus, the molar flux of H_2 through the membrane, J_{H_2} can be described by:

$$J_{H_2} = D\,\frac{\Delta C}{\delta} = D\,\frac{k_{H_2}\left(P_{H_2}^{ret}\right)^{0.5} - \left(P_{H_2}^{perm}\right)^{0.5}}{\delta} = L_{H_2}\,\frac{\left(P_{H_2}^{ret}\right)^{0.5} - \left(P_{H_2}^{perm}\right)^{0.5}}{\delta} \tag{3.28}$$

Where L_{H_2} = permeability coefficient of H_2

L_{H_2} through the Pd/SS membrane is expressed as a general Arrhenius expression:

$$L_{H_2} = L_{H_2,0}\,\exp\left(\frac{-\mathrm{E_P}}{\mathrm{RT}}\right) \tag{3.29}$$

Where $L_{H_2,O}$ = pre-exponential factor = 1.56×10^{-8} $m^3/m{\cdot}s{\cdot}Pa^{0.5}$ (Koffler et al., 1969)

E_P = activation energy of H_2 permeation = 15.7 kJ/mol (Koffler et al., 1969)

The H_2 molar flow rate through the Pd/SS membrane, $F_{H_2,perm}$ (kmol/h) which is resulted from J_{H_2} is then defined by:

$$\frac{dF_{H_2,perm}}{dL^*} = L_{H_2} \cdot 2\pi r_{Pd/SS} L \cdot \frac{\left(P_{H_2}^{ret}\right)^{0.5} - \left(P_{H_2}^{perm}\right)^{0.5}}{\delta} \tag{3.30}$$

Where $r_{Pd/SS}$ = outer radius of Pd/SS membrane

= membrane inner radius + membrane thickness

H_2 yield (Y_{H_2}) is defined by:

$$Y_{H_2} = \frac{Total\ moles\ of\ H_2\ produced}{F_{CH_4}^0}$$

$$= \frac{Moles\ of\ H_2\ produced\ at\ reaction\ zone}{F^0_{CH_4}} + \frac{Moles\ of\ H_2\ diffuse\ to\ permeate\ zone}{F^0_{CH_4}}$$

$$Y_{H_2} = \frac{F_{H_2}}{F^0_{CH_4}} + \frac{F_{H_2,perm}}{F^0_{CH_4}} \tag{3.31}$$

Let $Z_{H_2} = \frac{F_{H_2,perm}}{F^0_{CH_4}}$, equation (3.30) becomes:

$$\frac{dZ_{H_2}}{dL^*} = \frac{L_{H_2} \cdot 2\pi r_{Pd/SS} L}{F^0_{CH_4} \cdot \delta} \left[\left(P^{ret}_{H_2}\right)^{0.5} - \left(P^{perm}_{H_2}\right)^{0.5} \right] \tag{3.32}$$

Where $P^{ret}_{H_2}$ = Retentate side (Reaction zone) partial pressure of H_2 (bar)

$P^{perm}_{H_2}$ = Partial pressure of H_2 at permeate side (bar)

$$= \frac{F_{H_2,perm}}{F_{Sweep} + F_{H_2,perm}} \times P_{Perm}$$

P_{Perm} = Pressure of permeate zone (bar)

F_{Sweep} = Sweep gas flow rate at permeate zone (kmol/h)

The performance of MR is evaluated by the conversion of CH_4 (X_{CH_4}), yield of H (Y_{H_2}), CO Selectivity (S_{CO}) and CO_2 selectivity (S_{CO_2}), which are defined by:

$$X_{CH_4} = \frac{F_{CH_4,0} - F_{CH_4}}{F^0_{CH_4}} \times 100\% = \frac{\rho_b L A_C}{F^0_{CH_4}} (r_1 + r_3) \times 100\% \tag{3.33}$$

$$Y_{H_2} = Z_{H_2} + \frac{F_{H_2}}{F^0_{CH_4}} = \frac{F_{H_2,perm} + F_{H_2}}{F^0_{CH_4}}$$

$$= \left\{ \frac{L_{H_2} \cdot 2\pi r_{Pd/SS} L}{F^0_{CH_4} \cdot \delta} \left[\left(P^{ret}_{H_2}\right)^{0.5} - \left(P^{perm}_{H_2}\right)^{0.5} \right] \right\} + \left\{ \frac{\rho_b L A_C}{F^0_{CH_4}} (3r_1 + r_2 + 4r_3) \right\} \tag{3.34}$$

$$S_{CO_2} = \frac{F_{CO_2}}{F_{CO_2} + F_{CO}} \times 100\% \tag{3.35}$$

$$S_{CO} = \frac{F_{CO}}{F_{CO_2} + F_{CO}} \times 100\% \tag{3.36}$$

3.3 Kinetic Model

There is a general agreement that SMR reaction is first order in methane (Aguiar, 2002). The SMR reaction kinetics equation based on Ni/$MgAl_2O_4$ catalyst presented by Xu and Froment (1989) is well documented, gained wide acceptance and have been extensively used for SMR modelling in literature (Pantoleontos et al., 2012; Holt et al., 2018; Olivieri and Vegliò, 2008; Aguiar, 2002; Roux, 2011; Ayturk et al., 2009). The intrinsic rate equations for the three global SMR reaction are derived based on the Langmuir-Hinshelwood methodology, assuming the surface reaction is the rate-determining step among adsorption, surface reaction and desorption. Elnashaie et al., (1990) concluded that the kinetic model presented by Xu and Froment (1989) is more universal than the SMR kinetics proposed by other researchers. Therefore, kinetic model by Xu and Froment, 1989 is used to simulate the SMR process. The three reactions that represent the SMR are:

$CH_4 + H_2O \leftrightarrow CO + 3H_2$ (1) Steam methane reforming reaction

$CO + H_2O \leftrightarrow CO_2 + H_2$ (2) Water-gas shift reaction

$CH_4 + 2H_2O \leftrightarrow CO_2 + 4H_2$ (3) Reverse methanation

The rate equations for reaction (1) to (3) are tabulated in Table 3.3 below (Xu and Froment, 1989).

Table 3.3: Reaction rate equations.

j	Reaction rate (kmol/kg cat s)	Based on species
1	$r_1 = \frac{\frac{k_1}{P_{H_2}^{2.5}}\left(P_{CH_4}P_{H_2O} - \frac{P_{H_2}^3 P_{CO}}{K_{eq,1}}\right)}{(DEN)^2}$	r_1 = rate of formation of CH_4 in steam methane reforming reaction.
2	$r_2 = \frac{\frac{k_2}{P_{H_2}}\left(P_{CO}P_{H_2O} - \frac{P_{H_2}P_{CO_2}}{K_{eq,2}}\right)}{(DEN)^2}$	r_2 = rate of formation of CO in water-gas shift reaction.